Groundwater sapping as the cause of irreversible desertification of Hunshandake Sandy Lands, Inner Mongolia, northern China

Xiaoping Yang[a,1], Louis A. Scuderi[b,1], Xulong Wang[c], Louis J. Scuderi[d], Deguo Zhang[a], Hongwei Li[a], Steven Forman[e], Qinghai Xu[f], Ruichang Wang[g], Weiwen Huang[h], and Shixia Yang[h]

[a]Key Laboratory of Cenozoic Geology and Environment, Institute of Geology and Geophysics, Chinese Academy of Sciences, Beijing 100029, China; [b]Department of Earth and Planetary Sciences, University of New Mexico, MSC03 2040, Albuquerque, NM 87131; [c]Institute of Earth Environment, Chinese Academy of Sciences, Xian 710075, China; [d]Institute for Astronomy, University of Hawaii, Honolulu, HI 96822-1839; [e]Geoluminescence Dating Research Laboratory, Department of Geology, Baylor University, Waco, TX 78798; [f]College of Resources and Environment, Hebei Normal University, Shijiazhuang 050024, China; [g]Institute of Archaeology, Chinese Academy of Social Sciences, Beijing 100710, China; and [h]Institute of Vertebrate Paleontology and Paleoanthropology, Chinese Academy of Sciences, Beijing 100044, China

Edited by Thomas Dunne, University of California, Santa Barbara, Santa Barbara, CA, and approved December 5, 2014 (received for review September 19, 2014)

In the middle-to-late Holocene, Earth's monsoonal regions experienced catastrophic precipitation decreases that produced green to desert state shifts. Resulting hydrologic regime change negatively impacted water availability and Neolithic cultures. Whereas mid-Holocene drying is commonly attributed to slow insolation reduction and subsequent nonlinear vegetation–atmosphere feedbacks that produce threshold conditions, evidence of trigger events initiating state switching has remained elusive. Here we document a threshold event ca. 4,200 years ago in the Hunshandake Sandy Lands of Inner Mongolia, northern China, associated with groundwater capture by the Xilamulun River. This process initiated a sudden and irreversible region-wide hydrologic event that exacerbated the desertification of the Hunshandake, resulting in post-Humid Period mass migration of northern China's Neolithic cultures. The Hunshandake remains arid and is unlikely, even with massive rehabilitation efforts, to revert back to green conditions.

climate change | geomorphology | human activity | Holocene | geology

Earth's climate is subject to abrupt, severe, and widespread change, with nonlinear vegetation–atmosphere feedbacks that produced extensive and catastrophic ecosystem shifts and subsequent cultural disruption and dispersion during the Holocene (1–7). In the early and middle Holocene, northern China's eastern deserts, including much of the currently sparsely vegetated and semistabilized Hunshandake (Figs. 1 and 2), were covered by forests (8), reflecting significantly wetter climate associated with intensification of monsoon precipitation by up to 50% (6).

Monsoonal weakening, in response to middle-to-late Holocene insolation decrease, reduced precipitation, leading to a green/sandy shift and desertification across Inner Mongolia between ca. 5,000 and 3,000 y (years) ago (6). However, variations in the timing of this transition (9, 10) suggest local/regional thresholds or possibly environmental tipping by stochastic fluctuations. The impacts of this wet-to-dry shift in the Hunshandake, expressed as variations in surface and subsurface hydrology coincident with the termination of the formation of thick and spatially extensive paleosols, and the impacts of a ca. 4.2 ka (1 ka = 1,000 years) mid-Holocene desiccation of the Hunshandake on the development of early Chinese culture remain poorly understood and controversial (6, 11). Here we report for the first time to our knowledge on variability in a large early-to-middle Holocene freshwater lake system in China's Hunshandake Sandy Lands and associated vegetation change, which demonstrates a model of abrupt green/desert switching. We document a possible hydrologic trigger event for this switching and discuss associated vegetation and hydrologic disruptions that significantly impacted human activities in the region.

Paleolake System and Its Chronology

The spatial organization of Hunshandake dunes and interdune depressions indicates that current stabilized dune ridges with transverse and roughly concentric lunette-type forms are controlled by locations of former shorelines. Shoreline dune deposits from the three largest eastern Hunshandake lake basins (Figs. 2 and 3) and their degree of cementation suggest that they formed during lake recession and desiccation, with aeolian sands burying older, laminate lacustrine sediments. These lacustrine/shoreline facies include dark-colored and strongly cemented fine-grained sediments with abundant diatoms, the most common of which are *Pediastrum*, *Cyclotella*, and *Stephanodiscus*, typical of floating algae in freshwater lakes (*SI Appendix*, Table S1). These freshwater paleolakes are open systems with connecting channels and well-defined inlets and outlets that reflect flow between the basins during highstands (Fig. 2 and *SI Appendix*, Fig. S1). Drainage networks derived from a Shuttle Radar Topography Mission (SRTM) digital elevation model indicate that the lakes were recharged by inflows from rivers with headwaters to the south, i.e.,

Significance

In contrast to earlier assertions that deserts in northern China are 10^6 years old, our multidisciplinary investigation in the Hunshandake Sandy Lands, located in the eastern portion of China's desert belt, shows that this desert is ca. 4,000 years old. This study documents dramatic environmental and landscape changes in this desert during the last 10,000 years. For the first time to our knowledge we present a case of desertification mainly triggered by changes in the hydrological and geomorphological system, associated with climate change at ca. 4.2 ka. Our research on the human–environment interactions in the Hunshandake suggests Chinese civilization may be rooted in the marginal areas in the north, rather than in the middle reaches of the Yellow River.

Author contributions: X.Y. and L.A.S. designed research; X.Y., L.A.S., X.W., L.J.S., D.Z., H.L., S.F., Q.X., R.W., W.H., and S.Y. performed research; X.Y., L.A.S., and S.F. contributed new reagents/analytic tools; X.Y., L.A.S., X.W., L.J.S., D.Z., H.L., S.F., Q.X., R.W., W.H., and S.Y. analyzed data; X.Y. and L.A.S. wrote the paper; and X.W. and S.F. wrote the sections on dating methods. All authors shared ideas and results and helped produce the final manuscript.

The authors declare no conflict of interest.

This article is a PNAS Direct Submission.

Freely available online through the PNAS open access option.

[1]To whom correspondence may be addressed. Email: xpyang@mail.igcas.ac.cn or tree@unm.edu.

This article contains supporting information online at www.pnas.org/lookup/suppl/doi:10.1073/pnas.1418090112/-/DCSupplemental.

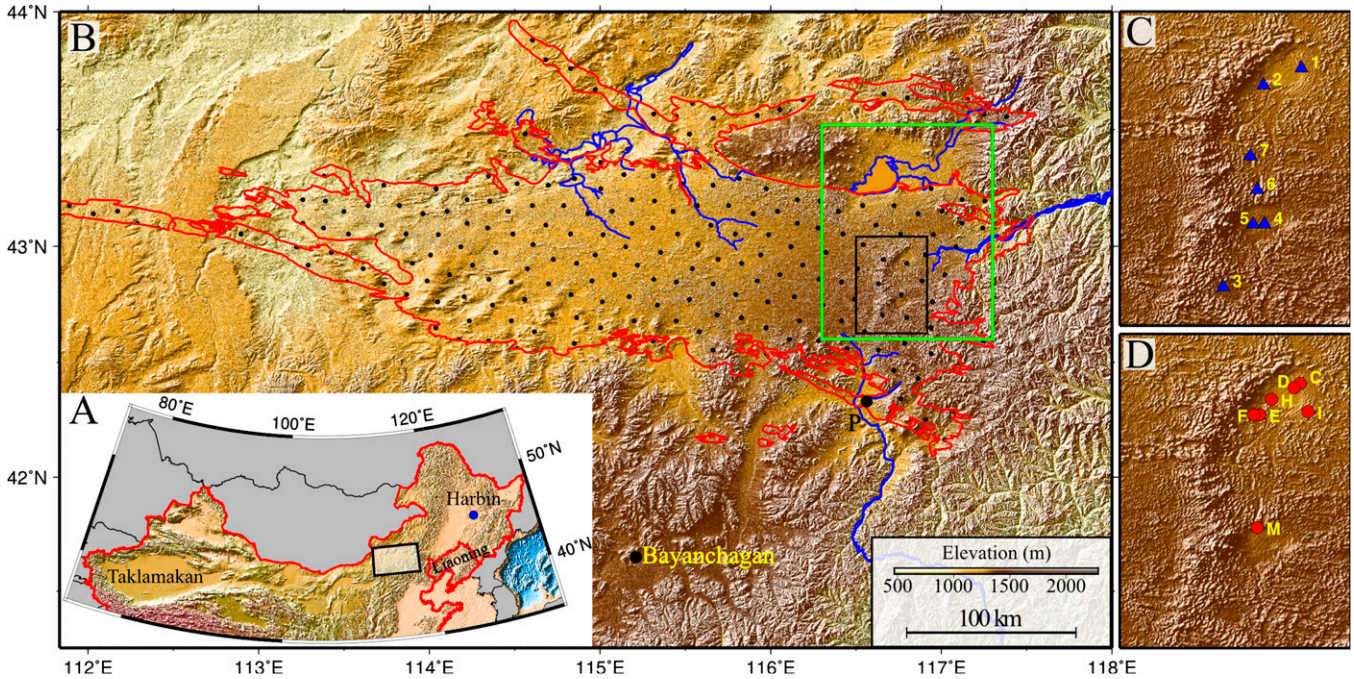

Fig. 1. Geographical location of the Hunshandake Sandy Lands (*A*) and its area (encircled by red line in *B*). The black rectangle in *B* marks the location of the enlarged maps *C* and *D* on the *Right*, and the green rectangle shows the location of Fig. 2. Map *C* shows the localities of water samples, and map *D* shows the localities of sections with stratigraphy presented in Fig. 3. The sand–paleosol section P (Fig. 3) is on the southern margin, and the site Bayanchagan marks the coring site of ref. 8. Rivers with headwaters in the Hunshandake likely formed by groundwater sapping are marked in blue. Drainages to the southwest and west are currently undergoing groundwater sapping, with substantial spring-driven flow found at the current river base level.

with a much larger catchment that produced surface flow during the wetter early-to-middle Holocene (see *SI Appendix*, Fig. S2).

Optically Stimulated Luminescence (OSL) dated highstands show that the earliest shorelines are early Holocene and formed at the beginning of Inner Mongolia's Humid Period. A prominent deflation surface at the northern lake exposes lacustrine sands (11.4 ± 0.6 ka) (Fig. 3, section E), suggesting an early initiation of lakes in the region. Lacustrine deposits exposed on the lake's eastern shore, OSL-dated to between 10.3 ± 0.6 and 9.3 ± 0.4 ka, and lacustrine sands in higher elevations that date to between 5.7 ± 0.3 and 5.2 ± 0.2 ka, indicate an increase in lake level from 1,324 to 1,340 m by 5 ka. Thick gray lacustrine sediments

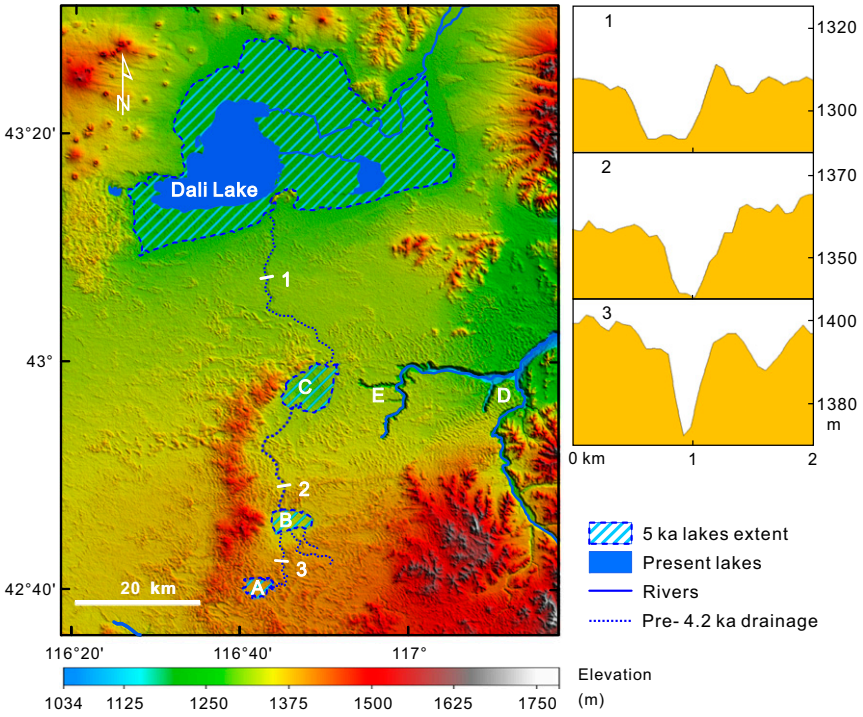

Fig. 2. (*Left*) Holocene lakes and channels in the Hunshandake and lake extent at selected epochs. Upper, middle, and lower lakes are indicated by points A, B, and C, respectively. Xilamulun River (point D) drains to the east. Groundwater-sapping headcuts at the upper reaches of incised canyons (point E) suggest a mid-Holocene interval of easterly surface flow, followed by groundwater drainage beginning at the ca. 4.2 ka event. Northern and central channels at point E are currently abandoned, and groundwater sapping has migrated to the southerly of the three channels shown. (*Right*) Cross-sections of the predrainage shift, northerly drainage into Dali Lake (Localities shown on the *Left*), showing the increase in widths of channels downstream (Vertical exaggeration ~30:1).

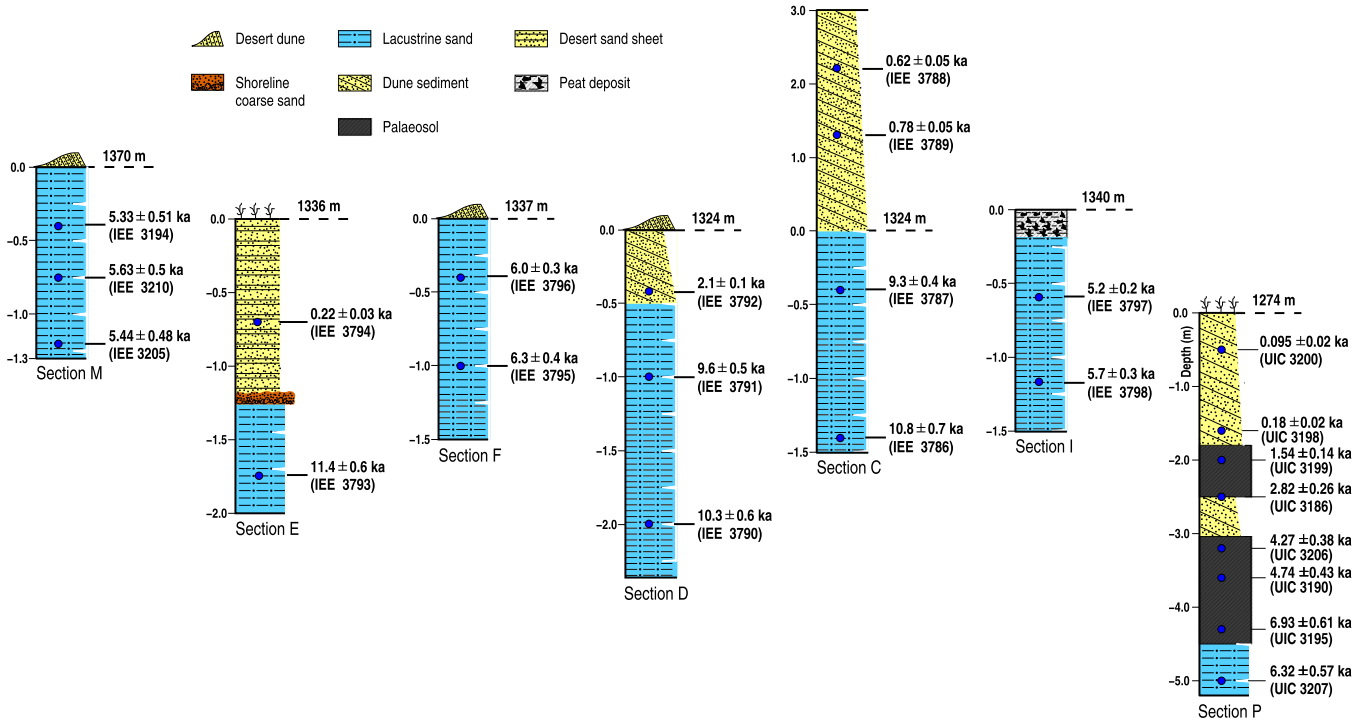

Fig. 3. Sedimentary profiles and their OSL chronologies along the former early-to-middle Holocene shoreline of the lower lake (E, F, D, C, and I) and middle lake (M) and section P in the southern margin of the Hunshandake (Fig. 1). IEE indicates the samples dated in the Institute of Earth Environment, Chinese Academy of Sciences, while UIC refers to the samples dated in the University of Illinois at Chicago.

suggest a prolonged and relatively deep-water environment between 9 and 5 ka (see *SI Appendix*, Fig. S3). Pollen from lake sediments and ^{14}C dating of preserved tree subfossils indicate the dominance of *Betula, Picea*, *Abies*, *Pinus*, and *Quercus*. However, during wet conditions in the early and middle Holocene, this area is characterized as temperate steppe environment, dominated by grasslands and trees near lakes and streams (8, 10, 12, 13).

Well-developed dark grassland-type paleosols (mollisols) at the southern edge of the Hunshandake, OSL-dated to between 6.93 ± 0.61 and 4.27 ± 0.38 ka (Fig. 3), also suggest a wetter climate. Lacustrine sands underlying this paleosol indicate an earlier wetland environment followed by soil formation that indicates a rapid transition to dry conditions at ca. 4.2 ka. Because the southern part of the Hunshandake was not impacted by ground water sapping until recently, it returned to green conditions again at ca. 2.8 ka and maintained this state for slightly longer than 1,000 y (Fig. 3, section P). Similarly, paleosols developed during the period between ca. 9.6 and ca. 3 ka in the western part of Hunshandake (6), where groundwater sapping has yet to occur. The total area of desertification since ca. 4.2 ka ago is >20,000 km^2 based on field observations and associated mapping.

Groundwater Sapping in the Hunshandake

A relict channel from the northern lake indicates that outflow before ca. 4.5 ka was directed 30 km north to megalake Dali (Fig. 2 and *SI Appendix*, Fig. S1). However, a lack of recessional shorelines, the presence of well-preserved terraces, and tributaries containing relict terraces and meander loops that grade eastward to an ancestral Xilamulun River ~50 m above the current base level (see *SI Appendix*, Fig. S4) suggest rapid and possibly catastrophic lake level decline, with a switch to east-flowing surface drainage ca. 4.2 ka. An increase in the coarse sand fraction in a lake basin core to the southeast, originally interpreted as a state shift response to a drying climate (10), also suggests a rapid transition to drier conditions by ca. 4.2 ka.

Narrow V-shaped canyons incised into thick sand and silt deposited by aeolian, fluvial, and lacustrine processes (Fig. 2 and *SI Appendix*, Fig. S1) indicate that groundwater sapping (14, 15) or seepage erosion (16) by the headcutting Xilamulun River captured the groundwater table and resulted in rapid lake level lowering. This large-scale hydrologic piracy breached multiple drainage divides, permanently diverting water resources into the east-flowing Xilamulun River. The presence of lacustrine sediments east of the lake basins studied suggests that this is an ongoing process, as the Xilamulun River rapidly headcut during the Holocene. Once eastward flow was established the water table dropped ~30 m to a level where surface flow was unsustainable, and rapid desertification ensued. Continued downcutting further lowered and steepened the water table's eastern slope, leaving tributaries in our study area, as well as drainages associated with paleolakes to the east, as dry canyons with present drainage from springs at river level and through groundwater sapping (Fig. 2).

Devastating Impact on the Hongshan Culture

The consequences of a rapid climatic/hydrologic state shift on the Hunshandake's mixed herding/agricultural Neolithic Hongshan and contemporaneous cultures were likely catastrophic. The Hongshan culture, established ~6,500 cal B.P.—over 3 millennia before the florescence of the Chinese Shang Dynasty—was first recognized 300 km east of our study sites in the river valleys and hills of western Liaoning Province in northeastern China (17). We found previously unreported abundant remnants of Hongshan pottery and microlithic and macrolithic stone tools preserved in early-to-middle Holocene lacustrine deposits and interbedded sandy layers of former shorelines (~9.0–5.2 ka) (see *SI Appendix*, Fig. S5 and Table S2) far to the west of the area traditionally assumed to be Hongshan.

The large number and variety of artifacts associated with these shoreline deposits suggest a relatively dense human population dependent on hunting and fishing. Artifacts indicative of post-Hongshan culture are absent at all sites examined until ca. 3.5 ka. This temporal lacuna suggests rapid abandonment and migration at the onset of desertification and indicates that these habitats were suitable only when conditions were exceptionally favorable during lake highstands. This conclusion is supported by recent studies that show a profound lack of artifacts in the region near the current Xilamulun River headwaters beginning ca. 4.2 ka and lasting for over 600 y (18, 19).

The Hongshan, possibly the earliest Chinese kingdom (17), has typically been viewed as a remote culture outside the key areas of early Chinese civilization. However, recent discoveries, including the Goddess Temple, jade artifacts with symmetrical designs, and remnants of sheep bones indicating trade with Mongolian sheepherders, suggest cultural complexity and stability, although the degree of complexity and links to other emergent Neolithic cultures in Mongolia and Central Asia are still under debate (17). In particular, the level of Hongshan jade-working is highly advanced and unique in early China (20). The first dragon-like symbol of Chinese culture is characterized in carved jade as a footless fish-like creature and may have originated with the Hongshan rather than with later Yellow River cultures (17). Other aquatic animals, such as fish, turtles, and ducks, are represented in jade carvings of the Hongshan culture (20). These aquatic-motif artifacts (see *SI Appendix*, Fig. S6) may indicate a cultural source related to the Hunshandake's hydrologic excess in the early/middle Holocene.

Discussion and Conclusions

In a global context, a major climatic shift occurred at ca. 4.2 ka, marking the transition from an early and middle Holocene thermal maximum to late-Holocene colder and more unstable climate conditions (21–23). In semiarid regions of the world, this event is commonly associated with evidence of hazardous drought. Although there is no consensus as to whether drought events around 4.2 ka recorded in various parts of the world were indeed synchronous, extraordinary drought appears to have occurred on all Northern Hemisphere continents within a century or two of 4.2 ka (24). Severe drought is well-documented at ca. 4.2 ka in the Middle East and northern Africa (25–27). Drying at around 4.2 ka is also related to abrupt deforestation in the western Mediterranean region (28) and to the reactivation of dune systems on the margins of the Sahara (29). On the Tibetan Plateau, ^{10}Be exposure ages on shoreline features of Lake Tangra Yumco indicate recession from a highstand of 143 m above the current lake at 4.3 ± 0.3 ka, associated with a weakening monsoon (30). Closer to the Hunshandake Sandy Lands, pollen records from the temperate steppe of northern China indicate a dominance of forests and a maximum in wet conditions between 8 and 4 ka, as well as noticeable decline in tree pollen at ca. 4 ka, associated with large-scale drying (8, 13).

The Hunshandake green/desert switch, similar to that found in the Sahara, occurred in conjunction with regional drying, as monsoonal flow decreased over the region (6, 8). However, unlike the Sahara, where a return to a green state may occur under a scenario with future wetter conditions and increased surface vegetation (31), reestablishment of a green Hunshandake is highly unlikely. We infer that in the Hundshandake, when the groundwater equilibrium state was altered with progressive sapping, the falling water table led to an eventual collapse in system hysteresis. The combination of factors at ca. 4.2 ka, including fluvial degradation by ~30 m and a similar drastic lowering of the water table, which led to the disappearance of lakes, coupled with a precipitous drop in monsoonal precipitation, resulted in a dominance of aeolian processes. This produced the extreme aridification of the Hunshandake observed since 4.2 ka. We note that increasing precipitation alone will not reverse this hydrologic deficit because the prior system hysteresis has collapsed (3, 32) (Fig. 4). Because the groundwater table appears to be associated with sediments delivered to and stored in the basin on glacial/interglacial timescales, it is possible that current conditions may persist until enhanced erosion during glacial climatic conditions leads to basin filling and reestablishment of a higher groundwater table.

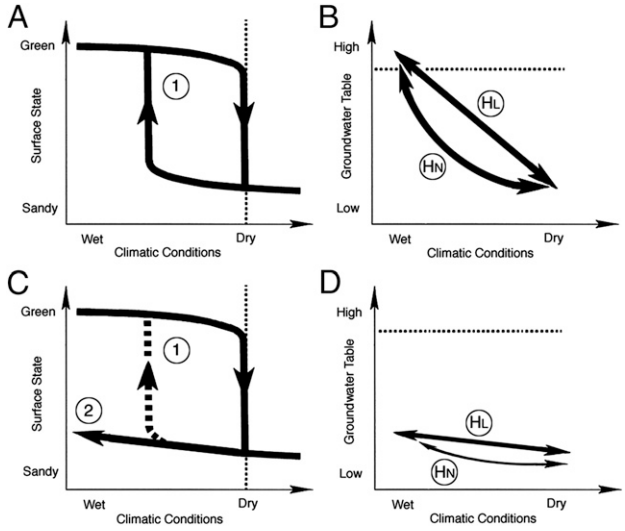

Fig. 4. Pathways by which the Sahara and Hunshandake responded to precipitation change induced by Holocene monsoonal penetration/strength variations. (*A*) As precipitation is reduced, the system moves toward a drier state, resulting in a state switch from green to desert. Subsequent wetter conditions result in a second state switch (pathway 1), with green conditions reestablished (the green switch occurs at precipitation levels indicated by the dotted vertical line in *A* and *C*). (*B*) Groundwater elevation change coincident with changing climate under a model where there are no constraints on groundwater levels. HL indicates a linear response, whereas HN is one of many possible nonlinear responses. (*C*) Alternative pathway 2, seen in the Hunshandake in response to a regional inability to maintain high groundwater levels due to drainage redirection and groundwater sapping because pathway 1 is no longer possible. Increased precipitation beyond currently documented Pleistocene/Holocene values (left of the *y* axis in the graph) results in removal of the sediments necessary to support a higher groundwater table. (*D*) Hydrologic responses, HL and HN, under all conditions no longer intersect the green state switch (dotted horizontal line in *B* and *D*) and are maintained at levels that cannot support a green Hunshandake.

Groundwater data also support our contention of a rapid and catastrophic state shift in the Hunshandake and continual lowering of the groundwater table and drying of the region. The mean tritium content of precipitation at Harbin, the closest International Atomic Energy Agency observation station, is ~30 TU, whereas tritium in groundwater from the study area wells varies from 2 to 24 TU (see *SI Appendix*, Table S3). These tritium concentrations indicate that groundwater in the eastern Hunshandake is just 1 to 2 decades old, with a short residence time in response to an eastward sloping groundwater table, reflecting headwater capture that began at ca. 4.2 ka. As headcutting and groundwater sapping expands westward, we expect that the freshwater and brackish lakes and salty pans of the western/central Hunshandake will continue to drain, further depleting near-surface groundwater and intensifying desertification (Fig. 1).

During the last decade the Hunshandake, widely viewed as a severe instance of human-induced desertification, has been the focus of intense rehabilitation efforts (33). However, our finding of an ecosystem tightly linked to irreversible regional geomorphic and hydrologic change suggests that these efforts may have limited success. Consequences of increased headwater erosion and groundwater sapping in this region include

continued ecological degradation and desertification. Our evidence suggests that Hongshan culture was devastated by the combined regional green/desert vegetation shift in the mid-Holocene, similar to that found in other monsoonal regions, but that that change was greatly intensified by the sudden north-to-east hydrologic shift ca. 4.2 ka, resulting from groundwater table drawdown by sapping. The Hunshandake's current population continues to be adversely impacted by that change today.

Methods

Between 2001 and 2014 we investigated landforms and sedimentary sequences throughout the Hunshandake Sandy Lands to determine aeolian and lacustrine late-Pleistocene/Holocene chronology as well as interactions between human activity and environmental change and their effects on the desertification processes. We dug numerous sedimentologic sections to refine our observations and to interpret the genesis of the sediments before collecting sand samples for luminescence dating from key sections. Sediments were identified as being of aeolian or fluvial/lacustrine origin based on bedding, cementation, color, and texture.

Luminescence dating was carried out using the OSL signal from extracted quartz. Samples for OSL dating were processed under subdued red light in both the Xian Luminescence Dating Laboratory of the Institute of Earth Environment, Chinese Academy of Sciences, China, and the Luminescence Dating Research Laboratory, University of Illinois at Chicago. All OSL measurements in Xian were performed using a Daybreak 2200 automated OSL reader equipped with a combined blue (470 ± 5 nm) and infrared (880 ± 80 nm) LED OSL unit and a $^{90}Sr/^{90}Y$ beta source (0.107 Gy/s) for irradiations. All luminescence measurements were made at 125 °C for 200 s, with both IR and blue stimulation powers being nominally ~45 mW/cm^2. Luminescence emissions were detected by an EMI 9235QA photomultiplier tube with two 3-mm-thick U-340 glass filters. The signal used for equivalent dose (D_e) determination was the integral for the first 5 s of the OSL decay curve. An Automated Risø TL/OSL-DA-15 system was used in Chicago. Blue-light excitation (470 ± 20 nm) was from an array of 30 light-emitting diodes that delivers ~15 mW/cm^2 to the sample position at 90% power. A Thorn EMI 9235 QA photomultiplier tube, coupled with three 3-mm-thick Hoya U-340 detection filters transmitting between 290 and 370 nm, measured photon emissions. Laboratory irradiations used a calibrated $^{90}Sr/^{90}Y$ beta source coupled with the Risø reader. The signals used for D_e determination were integrated over the first 0.8 s of stimulation out of 40 s of measurement, with background based on emissions for the last 30- to 40-s interval.

D_e value is determined by Single-aliquot Regenerative-dose (SAR) protocol (34) in both the Xian and Chicago laboratories. To identify diatoms in the lacustrine sediments, general and regional diatom floras as well as genera-specific references were consulted for identification. Digital photographs of all identified taxa were taken during counting to aid taxonomic consistency. The content of tritium was investigated to understand the residual time of the groundwater, and the analytical method of tritium followed Chinese National Standards (35). Geographic information system-based paleogeographical modeling of the megalake region used topographic maps, SRTM/Advanced Spaceborne Thermal Emission and Reflection Radiometer elevation data and Landsat satellite imagery were analyzed using spatial analysis tools in ARCMAP 10.1. Identification of Hongshan artifacts was based on shape, color, decoration, and materials.

For further details of laboratory procedures and data analysis, please see *SI Appendix, Additional Details of Methods*.

ACKNOWLEDGMENTS. Sincere thanks are extended to Professors Danian Ye, Baoying Yuan, Xingyou Tian, Xingcan Chen, and Xiaohong Zhang for discussions and to Professors Thomas Dunne and Martin Williams, anonymous reviewers, and editors for their very valuable comments on an earlier draft of this paper. This collaborative work was supported by the National Natural Science Foundation of China (Grants 41430532, 41172325, and 40930105) and the Chinese Academy of Sciences (Grant XDA05120502). L.A.S. thanks the Chinese Academy of Sciences for research support and the University of New Mexico for sabbatical leave support.

1. Claussen M, et al. (1999) Simulation of an abrupt change in Saharan vegetation in the mid-Holocene. *Geophys Res Lett* 26(14):2037–2040.
2. Foley JA, Coe MT, Scheffer M, Wang G (2003) Regime shifts in the Sahara and Sahel: Interactions between ecological and climatic systems in northern Africa. *Ecosystems (N Y)* 6(6):524–539.
3. Scheffer M, Carpenter S, Foley JA, Folke C, Walker B (2001) Catastrophic shifts in ecosystems. *Nature* 413(6856):591–596.
4. Higgins PAT, Mastrandrea MD, Schneider SH (2002) Dynamics of climate and ecosystem coupling: Abrupt changes and multiple equilibria. *Philos Trans R Soc Lond B Biol Sci* 357(1421):647–655.
5. Scheffer M, Carpenter SR (2003) Catastrophic regime shifts in ecosystems: Linking theory to observation. *Trends Ecol Evol* 18(12):648–656.
6. Yang X, et al. (2013) Initiation and variation of the dune fields in semi-arid northern China—with a special reference to the Hunshandake Sandy Land, Inner Mongolia. *Quat Sci Rev* 78:369–380.
7. Huang J, Wang S, Wen X, Yang B (2008) Progress in studies of the climate of Humid Period and the impacts of changing precession in early-mid Holocene. *Prog Nat Sci* 18(12):1459–1464.
8. Jiang W, et al. (2006) Reconstruction of climate and vegetation changes of Lake Bayanchagan (Inner Mongolia): Holocene variability of the East Asian monsoon. *Quat Res* 65(3):411–420.
9. Yang X, Scuderi LA (2010) Hydrological and climatic changes in deserts of China since the late Pleistocene. *Quat Res* 73(1):1–9.
10. Liu H, Xu L, Cui H (2002) Holocene history of desertification along the woodland-steppe border in northern China. *Quat Res* 57(2):259–270.
11. Jin G, Liu D (2002) Mid-Holocene climate change in North China and the effect on cultural development. *Chin Sci Bull* 47(5):408–413.
12. Cui H, Liu H, Yao X (1997) The finding of a paleo-spruce timber in Hunshandak Sandy Land and its paleoecological significance. *Science in China* 40(6):599–604.
13. Zhao Y, Yu Z (2012) Vegetation response to Holocene climate change in East Asian monsoon-margin region. *Earth Sci Rev* 113(1-2):1–10.
14. Laity JE, Malin MC (1985) Sapping processes and the development of theater-headed valley networks on the Colorado Plateau. *Geol Soc Am Bull* 96(2):203–217.
15. Howard AD, McLane CF (1988) Erosion of cohesionless sediment by groundwater seepage. *Water Resour Res* 24(10):1659–1674.
16. Dunne T (1990) Hydrology, mechanics, and geomorphic implications of erosion by subsurface flow. *Groundwater Geomorphology; The Role of Subsurface Water in Earth-Surface Processes and Landforms, Geol Soc of Am Spec Pap*, eds Higgins CG, Coates DR (Geol Soc of Am, Boulder, CO), 252:1–28.
17. Guo D (1985) *Hongshan Culture* (Artifacts Press, Beijing) (in Chinese).
18. Liu F, Feng Z (2012) A dramatic climatic transition at ~4000 cal. yr BP and its cultural responses in Chinese cultural domains. *Holocene* 22(10):1181–1197.
19. Wagner M, et al. (2013) Mapping of the spatial and temporal distribution of archaeological sites of northern China during the Neolithic and Bronze Age. *Quat Int* 290/291:344–357.
20. Anderson DC (2012) *Hongshan Jade Treasures: The Art, Iconography and Authentication of Carvings from China's Finest Neolithic Culture* (Tau Publishing, Fraz. Pian di Porto, Todi, Italy).
21. Bond G, et al. (2001) Persistent solar influence on North Atlantic climate during the Holocene. *Science* 294(5549):2130–2136.
22. Wanner H, Solomina O, Grosjean M, Ritz SP, Jetel M (2011) Structure and origin of Holocene cold events. *Quat Sci Rev* 30(21-22):3109–3123.
23. Geirsdóttir A, Miller G, Larsen DJ, Ólafsdóttir S (2013) Abrupt Holocene climate transitions in the northern North Atlantic region recorded by synchronized lacustrine records in Iceland. *Quat Sci Rev* 70:48–62.
24. Booth R, et al. (2005) A severe centennial-scale drought in mid-continental North America 4200 years ago and apparent global linkages. *Holocene* 15(3):321–328.
25. Bar-Matthews M, Ayalon A, Kaufman A (1997) Late Quaternary palaeoclimate in the eastern Mediterranean region from stable isotope analysis of speleothems at Soreq Cave, Israel. *Quat Res* 46(2):155–168.
26. Gasse F (2000) Hydrological changes in the African tropics since the Last Glacial Maximum. *Quat Sci Rev* 19(1-5):189–211.
27. Thompson LG, et al. (2002) Kilimanjaro ice core records: Evidence of Holocene climate change in tropical Africa. *Science* 298(5593):589–593.
28. Magri D, Parra I (2002) Late Quaternary western Mediterranean pollen records and African winds. *Earth Planet Sci Lett* 200(3-4):401–408.
29. Swezey C (2001) Eolian sediment responses to Late Quaternary climate changes: Temporal and spatial patterns in the Sahara. *Palaeog Palaeoc Palaeoe* 167(1-2): 119–155.
30. Rades EF, Hetzel R, Xu Q, Ding L (2013) Constraining Holocene lake-level highstands on the Tibetan Plateau by ^{10}Be exposure dating: A case study at Tangra Yumco, southern Tibet. *Quat Sci Rev* 82:68–77.
31. Janssen RHH, Meinders MBJ, van Nes EH, Scheffer M (2008) Microscale vegetation-soil feedback boosts hysteresis in a regional vegetation-climate system. *Glob Change Biol* 14(5):1104–1112.
32. Stocker TF, Marchal O (2000) Abrupt climate change in the computer: Is it real? *Proc Natl Acad Sci USA* 97(4):1362–1365.
33. Jiang H (2005) Grassland management and views of nature in China since 1949: Regional policies and local changes in Uxin Ju, Inner Mongolia. *Geoforum* 36(5): 641–653.
34. Murray AS, Wintle AG (2003) The single aliquot regenerative dose protocol: Potential for improvements in reliability. *Radiat Meas* 37(4-5):377–381.
35. State Environmental Protection Ministry (2004) *Analytical Method of Tritium in Water—GB 12375-90* (State Environ Protection Min of China, Beijing).